Tolerance of Intrinsic Defects in PbS Quantum Dots

4 AUTHORS, INCLUDING:

Danylo Zherebetskyy
Lawrence Berkeley National Laboratory
24 PUBLICATIONS **162** CITATIONS

SEE PROFILE

Lin-Wang Wang
Lawrence Berkeley National Laboratory
336 PUBLICATIONS **10,991** CITATIONS

SEE PROFILE

Tolerance of Intrinsic Defects in PbS Quantum Dots

Danylo Zherebetskyy,[†] Yingjie Zhang,[†,§] Miquel Salmeron,[†] and Lin-Wang Wang*,[†]

[†]Materials Sciences Division, Lawrence Berkeley National Laboratory, Berkeley, California 94720, United States
[§]Applied Science and Technology Graduate Program, University of California at Berkeley, Berkeley, California 94720, United States

(S) *Supporting Information*

ABSTRACT: Colloidal quantum dots exhibit various defects and deviations from ideal structures due to kinetic processes, although their band gap frequently remains open and clean. In this Letter, we computationally investigate intrinsic defects in a real-size PbS quantum dot passivated with realistic Cl-ligands. We show that the colloidal intrinsic defects are ionic in nature. Unlike previous computational results, we find that even nonideal, atomically nonstoichiometric quantum dots have a clean band gap without in-gap-states provided that quantum dots satisfy electronic stoichiometry.
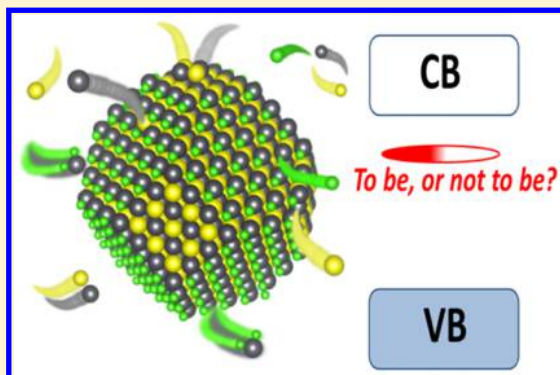
Colloidal semiconductor quantum dots (QDs) have attracted significant interest due to the easy tunability of their energy levels[1] and their potential application in low-cost solution-processed devices such as solar cells,[2,3] printable field effect transistors,[4,5] photodetectors, and light-emitting diodes.[6–8] The high performance of these QD-based devices relies sensitively on the absence of electronic trap-states within the band gap. However, the wet chemistry synthesis is not considered to be a high precision and highly controlled technique like the molecular beam epitaxy. Combining this fact with the large surface-to-volume ratios, one expects many intrinsic structural defects in the colloidal QDs, especially near the surface. It is of paramount importance to study the defect physical chemistry of QDs, and to see how the defects affect the electronic and optical properties of QDs, and how the situation is different from bulk semiconductors. As a matter of fact, despite the high likelihood of atomic defects, the electronic trap states for such systems, although sometimes experimentally observed,[5,9–13] are nevertheless not so abundant. Even in cases where in-gap states (IGSs) were experimentally observed, a recent study from our group[14] found that such IGSs were probably caused by external impurities, not by the intrinsic ones. Much of the success of QDs in many applications is partially owed to this tolerance of intrinsic defects. Here by intrinsic defect, we mean the removal of atoms and passivating ligands from ideally stoichiometric QD. QD atomic stoichiometry has been previously defined as $\Delta = -N_{\text{Pb(QD)}} + N_{\text{S(QD)}} + f N_{\text{LIG}}$, where $N_{\text{Pb(QD)}}$, $N_{\text{S(QD)}}$, N_{LIG} are the number of lead atoms, sulfur atoms, and ligands, f is the ligand weight factor describing the overall stoichiometry contribution of a single ligand; off-stoichiometry corresponds to $\Delta \neq 0$.[18] It has been argued that there is a self-healing process for QDs that drives intrinsic defects or external dopants to the QD surface.[15] Nevertheless, it is doubtful that such self-healing mechanism

can remove all the structural defects. Here we show that for IV−VI QDs, even if intrinsic defects—off stoichiometry—do exist, they do not produce any deep electronic IGS. This finding provides new mechanism to understand the relative lack of IGS in QDs, and demonstrates the electronic tolerance of QDs to the structural defects.

There have been several recent theoretical studies on the impact of defects and stoichiometric imbalance[16–18] on electronic structure, as well as the effect of ligand removal.[19,20]

Many previous theoretical studies have concluded that stoichiometric QDs are free from IGSs;[16–19] however, even a single deficiency of cation, anion, or ligand species will create highly localized IGSs;[16,18] if the imbalance becomes larger, these IGSs fill the band gap[16–20] and QDs become metallic.[16–20] These theoretical studies, combined with the likelihood of forming atomic defects might imply a large number of IGSs. Experimentally, electron microscopy images show numerous surface defects.[21] Although when IGSs are observed, their electronic levels have specific energy, and the whole band gap is never filled with IGSs.[12–14] This causes a contradiction and a puzzle between theory and experiment. However, in previous calculations, when one atom is removed, it is not the ion but the neutral atom that is removed. As we will show later, in a wet chemistry environment, it is often the ionic species, not the neutral atoms, that should be removed from a IV−VI QD. In the case of PbS, if one Pb atom is removed, it is most likely removed as Pb^{2+}, and, as a result, the nanocrystal will be bound with the counteranions in the solution.
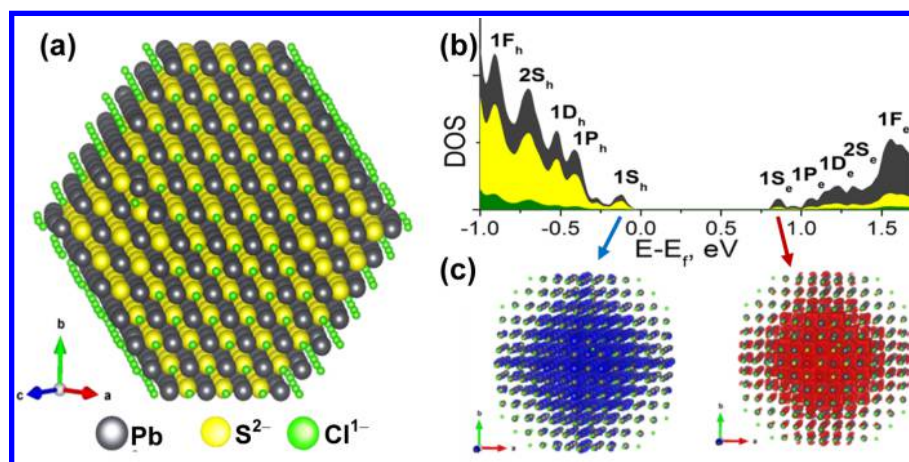
4711

Figure 1. (a) Optimized structure of Cl-passivated PbS-QD with 4 nm size and Wulff ratio of 0.87. (b) Partial density of states (DOS) for the constructed nanocrystal with 0.94 eV band gap, where the colors are consistent with that of the atoms in panel a. (c) Charge density distributions of the valence band maximum ($1S_h$) and conduction band minimum ($1S_e$).

Another problem that often hampers theoretical investigations of QD defects is the lack of a realistic atomic model of a passivated surface. As we showed in our recent work[21] on PbS QD, it is now possible to construct a detailed real ligand passivation model with ideal passivation without any IGS. In the present study, to simplify the situation, we will use a relatively simple, but still realistic model consisting of PbS quantum dots passivated by Cl atoms[3,22] and systematically introduce intrinsic structural defects (mostly vacancies). Our calculations show that (1) ionic defects, which are also charged defects, are energetically more preferable than the neutral defects; (2) interior ionic defects (especially the S defects) are driven off from the interior to the surface; and (3) ionic Pb and ligand defects do not introduce IGSs, while ionic S surface defects introduce very shallow states (~80 meV) near the conduction band minimum (CBM). All these indicate that either the intrinsic defects (with their proper charge state) do not induce deep electronic IGS states, or the ones that introduce IGS (S interior vacancy) will likely be removed and become shallow states. These results can explain why the Pb chalcogenide colloidal QDs have good electronic and optical properties despite the fact that it is almost impossible for the real QD to not have structural defects (especially at the surface).

For calculations, we used density functional theory (DFT) with a plane wave basis set as implemented in VASP computational code.[23−26] The computations employ the generalized gradient approximation (GGA) with Perdew and Wang (PW91)[27,28] exchange-correlation functional. The projected augmented wave (PAW) method of Blöchl[26,29] was used for the pseudopotential treatment. We used a kinetic energy cutoff of 300 eV. Ligands and the outmost atomic layer of QD are relaxed, while internal atoms are kept fixed. For defect calculations, all atoms in the first coordination sphere of a defect are also relaxed. Since QD is an isolated particle, only the gamma point was used to sample the Brillouin zone. The supercell contains a vacuum region of more than 8 Å to remove spurious interactions.

We begin our study with an ideally passivated PbS quantum dot (PbS-QD). This is aided by our previous theory and experimental study, and the new understanding of PbS-QD passivation with oleic acids and other ligands.[21] It was found both experimentally and theoretically that (1) the typical shape

of synthesized 4 nm PbS-QD is a truncated octahedron terminated by {100} and {111} planes;[21,30] (2) the Wulff ratio (h_{111}/h_{100}) of the truncated octahedron is ~0.85; (3) the Pb:S ion ratio is ~1.3:1; (4) the {111} facet can be passivated with oleate and hydroxide anions, the {100} facet does not require passivation, and the ligand-surface binding energy is very small; (5) the excess of Pb cations (relative to S anions) to oleate anions ratio is ~1:1; (6) edges and corners of the QD can also be passivated with small molecules; and (7) other small anions (like -Cl) can also be used as passivating agents. In order to simplify our calculations, we chose a relatively simple Cl-anion surface passivation that has been experimentally synthesized.[3,22] Rutherford backscattering spectroscopy (RBS) revealed that the Cl-ions and the excess Pb ions ratio is ~2.07:1 for 4 nm QD.[22] This is consistent with our theoretical understanding and the model of the PbS-QD structure. Since the formal charges of Pb and Cl are +2 and −1, respectively, one each excess Pb requires two Cl ions to passivate it. Taking into account that RBS uncertainty can exceed 2% and weakly-bound ligands on nonpolar {100} facets[21] can be easily washed away during the purification process, we can approximate that there are no Cl-surfactant species on nonpolar {100} facets. Based on this understanding, we have constructed a Cl-passivated PbS-QD model of 4 nm diameter. The system has a chemical formula $Pb_{586}S_{459}Cl_{254}$, a Wulff ratio of 0.87, a Pb:S ratio of 1.28:1 and a $Cl:Pb_{excess}$ ratio of 2.00:1 (Figure 1A).

We then optimized the geometry of the ligand layer (−Cl) and the outmost atomic layer of the idealized PbS-QD (Figure 1A). The calculated band gap of the optimized PbS-QD is 0.94 eV. This band gap is smaller than the experimentally-observed band gap of ~1.1 eV for 4 nm PbS-QDs[22] due to the well-known DFT underestimation of a semiconductor band gap.[31] The structure of the calculated DOS (Figure 1B) is very similar to that measured experimentally.[12,32] The valence band mainly consist of S(3p) orbitals with a smaller contribution from Pb(6s) and Cl(3p) orbitals, while the conduction band is predominantly of Pb(6p)-character. The valence band maximum (VBM) and CBM states are located in the interior of the QD (Figure 1C). Both states have only a small contribution from self-passivated {100} facets, while there is no contribution from the {111} facets. In terms of QD−QD coupling for charge transport from one QD to another, the unpassivated {100} facet will be much easier to be connected either by some other

linker molecules or in direct contact. This is in contrast with the well-passivated {111} facets where the surfaces are separated by the ligand molecules. Hence, cubic superlattices of assembled QDs ({100}−{100} interaction) should have better charge transport characteristics than hexagonal superlattices ({111}−{111} interaction).

Having solved the structure of the ideally Cl-passivated colloidal PbS-QD, we can investigate various intrinsic defects in the nanocrystal by removing atoms to form vacancies. The first question is in a real synthetic chemical environment,[33,34] will vacancies be neutral or charged defects? First, the neutral defect formation energies for Pb, S, and Cl vacancies are calculated and shown in Table S1. They all have large formation energies of about 2 eV. We next calculated the formation energies of the ionic vacancies (i.e., Pb^{2+}, S^{2-}, Cl^{1-}) that are all smaller than 1 eV (Tables S2−S4). The energies are calculated by assuming an overall chemical environment of the organic solvents during QD synthesis. However, the exact values have to be taken with caution due to the neglect of some terms, especially the entropy contributions. Nevertheless, from these calculations, the trend is clear: the ionic defects have much lower formation energies than their neutral defect counterparts.

Next, we considered various ionic vacancies. To simplify electronic structure calculations, unlike the defect formation energy calculations, we have not used any counterions for the charged QD with defects. Pb^{2+} vacancies are created by removing only a single Pb-ion from {100} and {111} facets and edges, corners, and from the QD interior. The structure of the defective QD is first optimized, and then its electronic structure is calculated. Surprisingly, none of the Pb^{2+}-vacancy defects create any trap-state within the band gap (Figure 2A). We next considered Cl^{1-} defects by removing ions from QD corner, {100} and {111} edges, middle, and randomly chosen cites on {111} facets. We relaxed the structures and calculated the density of states (Figure 2B). Again, none of Cl-ion defects produce IGSs. This also means the surface of PbS-QD does not require perfect passivation. This is a major difference from that of highly covalently bonded surfaces (e.g., IV−IV, III−V semiconductors) where any imperfection of the surface passivation or reconstructions will introduce dangling bond states in the band gap.

The situation of S^{2-} defects is different. Since {111}-facets do not contain surface S-ions, we removed S^{2-} only from the {100} facets and from the QD interior (third layer and QD center). In all three cases, an extra empty IGS is formed in addition to the original CBM state (Figure 2C). While the state energy is deep for the interior S^{2-} defects, for the surface S^{2-} defects the energy is almost the same as that of the original CBM state (only 80 meV lower). Thus, in terms of the band gap, there is not much change due to the surface S^{2-} defect whose state merges with the conduction band (Figure 2C). Figure 3 shows the CBM of the ideal QD as well as the S^{2-} defect-induced states of the defective QDs. We can see that wave functions of these defect states occupy a large portion of the QD volume. We have also investigated S^{2-} vacancy in bulk PbS, and a similar defect state is found. As discussed above, the calculated absolute formation energies for these defect states (Table S4) might be inaccurate due to the difficulty in calculating the solvent energies, but the difference in formation energies among the three defect locations (Table S4) are not affected by this uncertainty (they have the same solvent energy). As we can see, there is a major energy drive of ~0.90 eV to move the defect from QD center toward the {100}
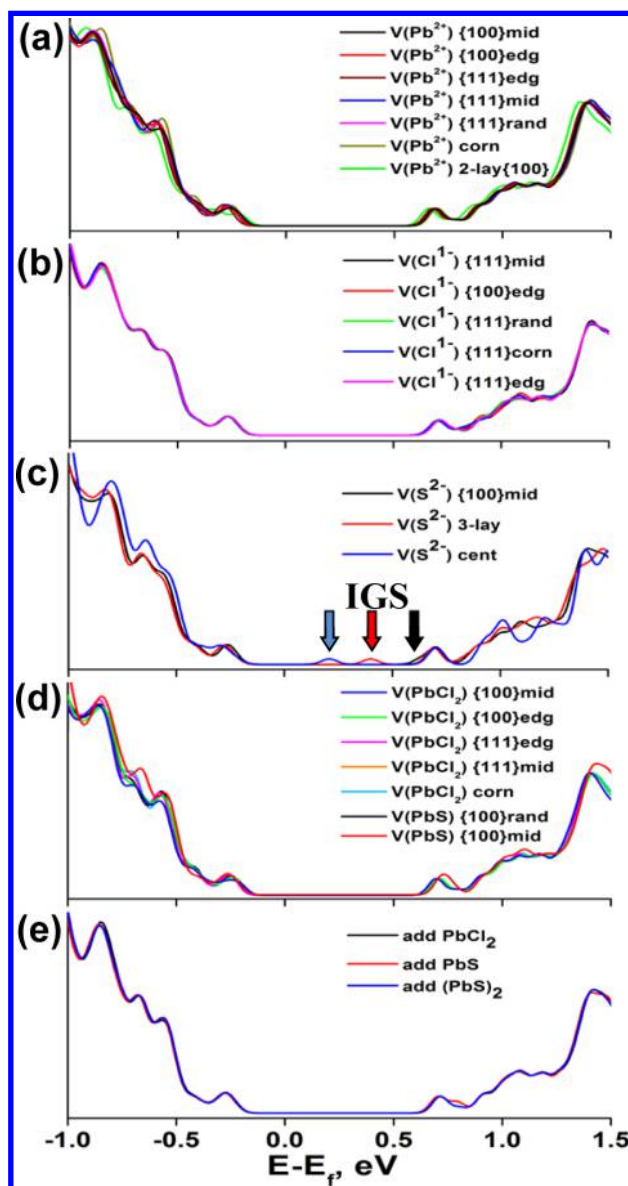

Figure 2. Density of states for colloidal intrinsic ionic defects in a 4 nm Cl-passivated PbS-QD for (a) Pb^{2+} vacancy defects, (b) Cl^{1-} vacancy defects, (c) S^{2-} vacancy defects, (d) charge-balanced $Pb^{2+}Cl^{1-}_2$ and $Pb^{2+}S^{2-}$ vacancy defects, (e) adsorption of $PbCl_2$, PbS and $(PbS)_2$ complexes representing adatoms and islands. Notation: V - vacancy defects; add - adsorption defects; {100} - on {100} facet; {111} - on {111} facet; edg - on an edge; mid - in a facet's middle; rand - random; cent - in QD center; corn - in QD corner; n-lay - nth layer under facet. Only S-ion vacancies produce IGS in the upper half of the band gap (near CBM).

surface. To further investigate whether this energy drive can indeed move the S^{2-} defect, we have calculated the vacancy diffusion barrier using a nudged elastic band (NEB) method for a bulk S^{2-} vacancy. We found that the barrier height is about 1.14 eV. On the other hand, since there is about 0.90 eV energy drop from the center vacancy to the edge vacancy (with 4 hop steps), there is a 0.225 eV energy drop for each hop. In the harmonic approximation, this energy drop lowers the barrier height to $\Delta E = 1.03$ eV (see Supporting Information (SI)). Using the Eyring equation, we can estimate the rate constant $r = (kT/h)(q_{TS}/q_{GS}) \exp(-(\Delta E/kT))$. The partition function ratio q_{TS}/q_{GS} is estimated to be 14.7×10^{-3} (see SI), and hence,
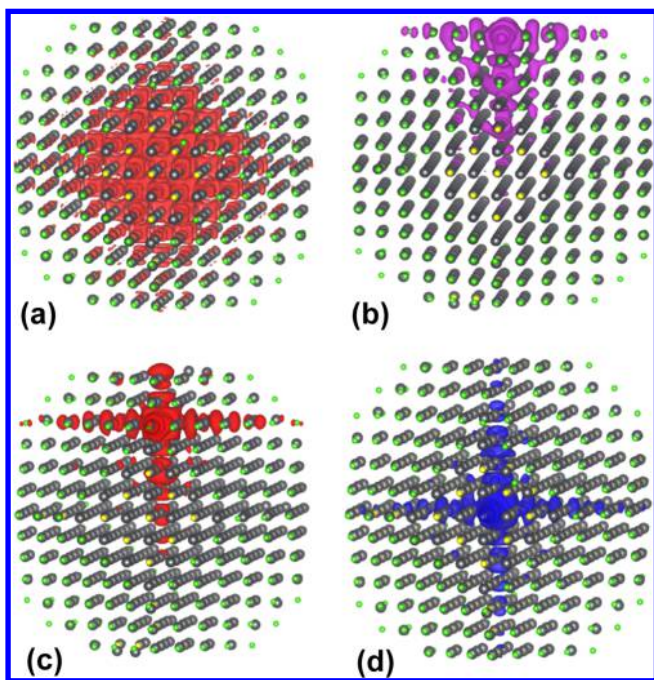
Figure 3. Charge density distributions for CBM of an ideal QD (a), and IGS of a QD with ionic S^{2-} vacancies in the {100} facet (b), in the third layer under {100} (c), and in the QD-center (d). Isosurface values are 1.5%. Defect states are significantly delocalized within the QD.

at the experimental synthesis temperature of 135 °C we can estimate the hopping time of the S^{2-} vacancy toward the QD surface as $\tau \approx 40$ s. Thus, the S^{2-} vacancy should be mobile and can move fairly quickly from the QD interior to the surface, and become a surface vacancy. This self-healing process can thus change a deep IGS state into a shallow IGS state, reducing QD deterioration effects significantly. It is interesting to note that the calculated Pb^{2+} vacancy diffusion barrier (1.86 eV) is much higher, and, as a result, this vacancy is essentially immobile. Nevertheless, the Pb^{2+} vacancy, regardless of its position in the QD, will not induce any IGSs.

Since S^{2-} surface vacancies create IGS and have the smallest formation energies (Table S4), the S^{2-} surface vacancies can be potential surface trap states that quench photoluminescence. Obviously, a larger QDs will have larger probability of forming one such state per QD. This seems to agree with the observation of Semonin et al.[35] that smaller PbS and PbSe QDs have better quantum yields compared to larger ones, despite the fact they have larger surface/volume ratio. This also agrees with the experimental observation by Sun et al.[36] that a surface treatment by trioctylphosphine (TOP) can significantly improve the electrogenerated chemiluminescence (ECL). This is because the TOP can bind with S to form a surface TOPS, which stabilizes the surface S, and hence reduces the likelihood of surface S vacancies.

Besides single atomic/ionic defects, we have also investigated vacancy defects of stoichiometric atom pairs resulting in neutral QDs. We first remove an atom pair of $PbCl_2$ from different locations at the surface. Once again, no IGS is found (Figure 2D). Surface PbS defects do not induce any IGS (Figure 2D) either, while interior PbS defects produce an IGS (Figure S2), similar to the S^{2-} defects. Another similarity is the fact that the interior PbS defect has much larger formation energy (by 0.63 eV) than the surface PbS defect, which drives it to the surface.

Finally, opposite to the vacancies, it is interesting to study the adsorption of small molecular species on the QD surface, because atomic resolution transmission electron microscopy (TEM) images show that surface islands or additional single precursors often exist on the QD surface.[21] We have considered defects formed due to the adsorption of Pb-precursor ($PbCl_2$), one PbS pair, and two PbS pairs (($PbS)_2$ island) on a {100}-facet. They all have negative absorption energies, indicating that their absorption is favorable. However, the calculated band gap remains clean for all of the adsorption defects (Figure 2E). This means that there is no need to have an ideal geometry at the surface in order to have a clean band gap without IGS. Our finding that no IGS are formed from ionic surface vacancies is in line with our previous finding for ionic nonpolar oxides surfaces.[37] There we found that if the edge of the bulk conduction band consists mostly of transition metal d-states, while the edge of the bulk valence band consists mostly of O-2p states, then a nonpolar surface will not have IGS after atomic relaxation. For PbS, the bulk conduction band edge arises mostly from Pb states, while the bulk valence band edge arises mostly from S states. In such an ionic material, the properly charged ionic defects tend not to introduce IGS. Removal of Pb^{2+}, S^{2-} and charged ligands (Cl^{1-}) can be viewed as a way to maintain the overall electronic stoichiometry. Our new insight is that there is no IGS if QD preserves electronic stoichiometry of ions (i.e., the number of net charge in a QD should correspond to the ionic counting: $Q_{QD} = Q_{Pb} N_{Pb(QD)} + Q_S N_{S(QD)} + Q_{LIG} N_{LIG}$, where Q and N are the charge and number of Pb-cations, S-anions, and charged ligands, respectively, the total charge Q_{QD} can be nonzero, and in reality the QD can be further compensated by a counter charged ion from the solvent. This requirement is more general and inclusive, with $Q_{QD} = 0$ as a subclass, e.g., Voznyy et al.[16] and Kim et al.[18] found no IGS if the QD preserves atomic stoichiometry ($\Delta = 0$). Our requirement reflects the ionic nature of the QD and explains the good electronic properties of QD despite many structural defects. Nevertheless, it is possible to create n-type and p-type doping by introducing external defects using, for example, thermal vapor deposition of elemental Pb^0 and S^0 adatoms,[38] respectively: gas phase atoms cannot change to the ionic charge state. Pb^0 doping introduces two degenerate singly occupied states 0.36 eV below CBM. S^0 doping introduces three shallow partially occupied states within 0.1 eV above the VBM (Figure S1). These IGS have Fermi energy pinned at those IGSs, which will make the QD heavily doped, which lies in line with recent experiments;[13,38] thus, their effects will be significant.

Tang et al.[3] found that the QD surface can be passivated much better using halides than the large organic ligands, as halide passivation reduces the IGSs. While our calculations indicate that a single charged ionic defect will not introduce IGSs, if there are many such defects aggregated together, it is still likely they can introduce IGSs. This is because such defects are charged, and it is difficult to have electrostatic compensation from the environment for large aggregations of such defects. Thus, although perfect passivation might not be necessary, good passivation like the one provided by halides will still be necessary. Also note that if the neutral defects are formed, instead of the ionic defects, Pb, Cl and S vacancies will have IGSs as shown in Figure S2. These IGSs are also close to the band edge with the Fermi energy pinned at those IGSs, making QD heavily doped. Single defects that introduce IGSs in the band gap are summarized in Figure 4 to guide the interpretation of experimental measurements.
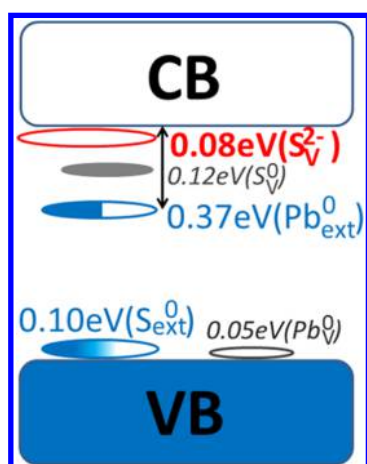
Figure 4. Schematic summary of the surface defect energy levels relative to nearest electronic bands. Notations: VB/CB - valence/conduction band; filled/empty shapes - occupied/unoccupied states (Pb^0_{ext} two degenerate half-occupied states); superscript - element charge; V - vacancy; ext - extra-atom on surface. Low-probability defects are denoted by smaller fonts.

In summary, we have used ab initio calculations to investigate various colloidal intrinsic vacancy defects and imperfect surface passivations of PbS QDs with the goal of explaining why experimentally there could be so few IGSs in structurally-imperfect QDs, in contrast to previous theoretical works.[16−20] The recent development and understanding of the PbS QD surface passivation allows us to start the investigation of a QD with realistic surface passivation. We emphasize that the vacancies in colloidal solution come from removal of ion species, instead of neutral atoms (due to the large differences in formation energy). We discovered that among all the intrinsic defects studied, only S^{2-} vacancies at the interior of the QD introduce deep IGS, while surface S^{2-} vacancies introduce very shallow IGS. Moreover, the S^{2-} vacancies at the interior have a higher formation energy compared to their surface counterparts. With a low diffusion barrier, we find that interior S^{2-} vacancies can diffuse to the surface within tens of seconds. Thus, overall, we should not see IGS created by intrinsic defects in PbS QDs. We also note that, experimentally, an IGS near the VBM has been observed in many QD films.[5−12] However, another study from our group, using both experimental and theoretical means, indicates that such IGS are induced by external molecules, not by intrinsic defects.[14] QDs prefer to maintain electronic stoichiometry, and the lack of IGSs induced by intrinsic defects or imperfection of passivation are the reasons why the general electronic quality of such colloidal QDs is good, regardless of the various possible nonideal atomic configurations.

ASSOCIATED CONTENT

Ⓢ Supporting Information

The Supporting Information is available free of charge on the ACS Publications website at DOI: 10.1021/acs.jpclett.5b02202.

> Formation energies of neutral and ionic defects, density of states for neutral defects, and PbS interior defect (PDF)

AUTHOR INFORMATION

Corresponding Author

*Address: Materials Sciences Division, Lawrence Berkeley National Laboratory, Berkeley, CA 94720. E-mail: lwwang@lbl.gov.

Author Contributions

The manuscript was written through contributions of all authors. All authors have given approval to the final version of the manuscript.

Notes

The authors declare no competing financial interest.

ABBREVIATIONS

QD-quantum dot; VBM-valence band maximum; CBM-conduction band minimum; DOS-density of states; IGS-in-gap-state

REFERENCES

(1) Alivisatos, A. P. Semiconductor Clusters, Nanocrystals, and Quantum Dots. *Science* **1996**, *271*, 933−937.

(2) Luther, J. M.; Gao, J.; Lloyd, M. T.; Semonin, O. E.; Beard, M. C.; Nozik, A. J. Stability Assessment on a 3% Bilayer PbS/ZnO Quantum Dot Heterojunction Solar Cell. *Adv. Mater.* **2010**, *22*, 3704−3707.

(3) Tang, J.; Kemp, K. W.; Hoogland, S.; Jeong, K. S.; Liu, H.; Levina, L.; Furukawa, M.; Wang, X.; Debnath, R.; Cha, D.; et al. Colloidal-Quantum-Dot Photovoltaics Using Atomic-Ligand Passivation. *Nat. Mater.* **2011**, *10*, 765−771.

(4) Mentzel, T. S.; Porter, V. J.; Geyer, S.; MacLean, K.; Bawendi, M. G.; Kastner, M. A. Charge Transport in PbSe Nanocrystal Arrays. *Phys. Rev. B: Condens. Matter Mater. Phys.* **2008**, *77*, 075316.

(5) Talapin, D. V.; Murray, C. B. PbSe Nanocrystal Solids for N- and P-Channel Thin Film Field-Effect Transistors. *Science* **2005**, *310*, 86−89.

(6) Steckel, J. S.; Coe-Sullivan, S.; Bulović, V.; Bawendi, M. G. 1.3μm to 1.55μm Tunable Electroluminescence from PbSe Quantum Dots Embedded within an Organic Device. *Adv. Mater.* **2003**, *15*, 1862−1866.

(7) Sun, Q.; Wang, Y. A.; Li, L. S.; Wang, D.; Zhu, T.; Xu, J.; Yang, C.; Li, Y. Bright, Multicoloured Light-Emitting Diodes Based on Quantum Dots. *Nat. Photonics* **2007**, *1*, 717−722.

(8) Kim, J. Y.; Voznyy, O.; Zhitomirsky, D.; Sargent, E. H. 25th Anniversary Article: Colloidal Quantum Dot Materials and Devices: A Quarter-Century of Advances. *Adv. Mater.* **2013**, *25*, 4986−5010.

(9) Nagpal, P.; Klimov, V. I. Role of Mid-Gap States in Charge Transport and Photoconductivity in Semiconductor Nanocrystal Films. *Nat. Commun.* **2011**, *2*, 486.

(10) Liu, Y.; Gibbs, M.; Puthussery, J.; Gaik, S.; Ihly, R.; Hillhouse, H. W.; Law, M. Dependence of Carrier Mobility on Nanocrystal Size and Ligand Length in PbSe Nanocrystal Solids. *Nano Lett.* **2010**, *10*, 1960−1969.

(11) Luther, J. M.; Law, M.; Song, Q.; Perkins, C. L.; Beard, M. C.; Nozik, A. J. Structural, Optical, and Electrical Properties of Self-Assembled Films of PbSe Nanocrystals Treated with 1,2-Ethanedithiol. *ACS Nano* **2008**, *2*, 271−280.

(12) Diaconescu, B.; Padilha, L.; Nagpal, P.; Swartzentruber, B.; Klimov, V. Measurement of Electronic States of PbS Nanocrystal Quantum Dots Using Scanning Tunneling Spectroscopy: The Role of Parity Selection Rules in Optical Absorption. *Phys. Rev. Lett.* **2013**, *110*, 127406.

(13) Bozyigit, D.; Volk, S.; Yarema, O.; Wood, V. Quantification of Deep Traps in Nanocrystal Solids, Their Electronic Properties, and Their Influence on Device Behavior. *Nano Lett.* **2013**, *13*, 5284−5288.

(14) Zhang, Y.; Zherebetskyy, D.; Barja, S.; Lichtenstein, L.; Bronstein, N. D.; Alivisatos, A. P.; Wang, L.-W.; Salmeron, M. Molecular Oxygen Induced In-Gap States in PbS Quantum Dots. *ACS Nano* **2015**, *9*, 10445−10452.

(15) Dalpian, G.; Chelikowsky, J. Self-Purification in Semiconductor Nanocrystals. *Phys. Rev. Lett.* **2006**, *96*, 226802.

(16) Voznyy, O.; Zhitomirsky, D.; Stadler, P.; Ning, Z.; Hoogland, S.; Sargent, E. H. A Charge-Orbital Balance Picture of Doping in Colloidal Quantum Dot. *ACS Nano* **2012**, *6*, 8448−8455.

(17) Wei, H. H.-Y.; Evans, C. M.; Swartz, B. D.; Neukirch, A. J.; Young, J.; Prezhdo, O. V.; Krauss, T. D. Colloidal Semiconductor Quantum Dots with Tunable Surface Composition. *Nano Lett.* **2012**, *12*, 4465−4471.

(18) Kim, D.; Kim, D.-H.; Lee, J.-H.; Grossman, J. C. Impact of Stoichiometry on the Electronic Structure of PbS Quantum Dots. *Phys. Rev. Lett.* **2013**, *110*, 196802.

(19) Ip, A. H.; Thon, S. M.; Hoogland, S.; Voznyy, O.; Zhitomirsky, D.; Debnath, R.; Levina, L.; Rollny, L. R.; Carey, G. H.; Fischer, A.; et al. Hybrid Passivated Colloidal Quantum Dot Solids. *Nat. Nanotechnol.* **2012**, *7*, 577−582.

(20) Voznyy, O.; Sargent, E. H. Atomistic Model of Fluorescence Intermittency of Colloidal Quantum Dots. *Phys. Rev. Lett.* **2014**, *112*, 157401.

(21) Zherebetskyy, D.; Scheele, M.; Zhang, Y.; Bronstein, N.; Thompson, C.; Britt, D.; Salmeron, M.; Alivisatos, P.; Wang, L.-W. Hydroxylation of the Surface of PbS Nanocrystals Passivated with Oleic Acid. *Science* **2014**, *344*, 1380−1384.

(22) Moreels, I.; Lambert, K.; Smeets, D.; De Muynck, D.; Nollet, T.; Martins, J. C.; Vanhaecke, F.; Vantomme, A.; Delerue, C.; Allan, G.; et al. Size-Dependent Optical Properties of Colloidal PbS Quantum Dots. *ACS Nano* **2009**, *3*, 3023−3030.

(23) Kresse, G.; Hafner, J. Ab Initio Molecular Dynamics for Liquid Metals. *Phys. Rev. B: Condens. Matter Mater. Phys.* **1993**, *47*, 558−561.

(24) Kresse, G.; Furthmuller, J. Efficiency of Ab-Initio Total Energy Calculations for Metals and Semiconductors using a Plane-Wave Basis Set. *Comput. Mater. Sci.* **1996**, *6*, 15−50.

(25) Kresse, G.; Furthmuller, J. Efficient Iterative Schemes for *Ab Initio* Total-Energy Calculations Using a Plane-Wave Basis Set. *Phys. Rev. B: Condens. Matter Mater. Phys.* **1996**, *54*, 11169.

(26) Kresse, G.; Joubert, D. From Ultrasoft Pseudopotentials to the Projector Augmented-Wave Method. *Phys. Rev. B: Condens. Matter Mater. Phys.* **1999**, *59*, 1758−1775.

(27) Perdew, J.; Chevary, J.; Vosko, S.; Jackson, K.; Pederson, M.; Singh, D.; Fiolhais, C. Atoms, Molecules, Solids, and Surfaces: Applications of the Generalized Gradient Approximation for Exchange and Correlation. *Phys. Rev. B: Condens. Matter Mater. Phys.* **1992**, *46*, 6671−6687.

(28) Perdew, J.; Wang, Y. Accurate and Simple Analytic Representation of the Electron-Gas Correlation Energy. *Phys. Rev. B: Condens. Matter Mater. Phys.* **1992**, *45*, 13244−13249.

(29) Blöchl, P. E. Projector Augmented-Wave Method. *Phys. Rev. B: Condens. Matter Mater. Phys.* **1994**, *50*, 17953−17979.

(30) Choi, H.; Ko, J.-H.; Kim, Y.-H.; Jeong, S. Steric-Hindrance-Driven Shape Transition in PbS Quantum Dots: Understanding Size-Dependent Stability. *J. Am. Chem. Soc.* **2013**, *135*, 5278−5281.

(31) Kurth, S.; Perdew, J. P.; Blaha, P. Molecular and Solid-State Tests of Density Functional Approximations: LSD, GGAs, and Meta-GGAs. *Int. J. Quantum Chem.* **1999**, *75*, 889−909.

(32) Liljeroth, P.; van Emmichoven, P.; Hickey, S.; Weller, H.; Grandidier, B.; Allan, G.; Vanmaekelbergh, D. Density of States Measured by Scanning-Tunneling Spectroscopy Sheds New Light on the Optical Transitions in PbSe Nanocrystals. *Phys. Rev. Lett.* **2005**, *95*, 086801.

(33) Murray, C.; Kagan, C.; Bawendi, M. Synthesis and Characterization of Monodisperse Nanocrystals and Close-Packed Nanocrystal Assemblies. *Annu. Rev. Mater. Sci.* **2000**, *30*, 545−610.

(34) Liu, H.; Owen, J. S.; Alivisatos, A. P. Mechanistic Study of Precursor Evolution in Colloidal Group II-VI Semiconductor Nanocrystal Synthesis. *J. Am. Chem. Soc.* **2007**, *129*, 305−312.

(35) Semonin, O. E.; Johnson, J. C.; Luther, J. M.; Midgett, A. G.; Nozik, A. J.; Beard, M. C. Absolute Photoluminescence Quantum Yields of IR-26 Dye, PbS, and PbSe Quantum Dots. *J. Phys. Chem. Lett.* **2010**, *1*, 2445−2450.

(36) Sun, L.; Bao, L.; Hyun, B.-R.; Bartnik, A. C.; Zhong, Y.-W.; Reed, J. C.; Pang, D.-W.; Abruña, H. D.; Malliaras, G. G.; Wise, F. W. Electrogenerated Chemiluminescence from PbS Quantum Dots. *Nano Lett.* **2009**, *9*, 789−793.

(37) Zherebetskyy, D.; Wang, L.-W. In-Gap States in Electronic Structure of Nonpolar Surfaces of Insulating Metal Oxides. *Adv. Mater. Interfaces* **2014**, *1*, 1300131.

(38) Oh, S. J.; Berry, N. E.; Choi, J.-H.; Gaulding, E. A.; Paik, T.; Hong, S.-H.; Murray, C. B.; Kagan, C. R. Stoichiometric Control of Lead Chalcogenide Nanocrystal Solids to Enhance Their Electronic and Optoelectronic Device Performance. *ACS Nano* **2013**, *7*, 2413−2421.